



UNIVERSITY OF LEEDS

This is a repository copy of *High-resolution imaging and monitoring of animal tunnels using 3D ground-penetrating radar*.

White Rose Research Online URL for this paper:
<http://eprints.whiterose.ac.uk/146137/>

Version: Accepted Version

Article:

Allroggen, N, Booth, AD orcid.org/0000-0002-8166-9608, Baker, SE et al. (2 more authors) (2019) High-resolution imaging and monitoring of animal tunnels using 3D ground-penetrating radar. *Near Surface Geophysics*, 17 (3). pp. 291-298. ISSN 1873-0604

<https://doi.org/10.1002/nsg.12039>

© 2019 European Association of Geoscientists & Engineers. This is an author produced version of a paper published in *Near Surface Geophysics*. Uploaded in accordance with the publisher's self-archiving policy.

Reuse

Items deposited in White Rose Research Online are protected by copyright, with all rights reserved unless indicated otherwise. They may be downloaded and/or printed for private study, or other acts as permitted by national copyright laws. The publisher or other rights holders may allow further reproduction and re-use of the full text version. This is indicated by the licence information on the White Rose Research Online record for the item.

Takedown

If you consider content in White Rose Research Online to be in breach of UK law, please notify us by emailing eprints@whiterose.ac.uk including the URL of the record and the reason for the withdrawal request.



eprints@whiterose.ac.uk
<https://eprints.whiterose.ac.uk/>

High resolution imaging and monitoring of animal tunnels using 3D ground-penetrating radar

Niklas Allroggen* (Institut für Geowissenschaften, Universität Potsdam, Karl-Liebknecht Straße 24, 14476 Potsdam, Germany)

5 Adam Booth (School of Earth and Environment, University of Leeds, Leeds, LS2 9JT, UK)

Sandra E. Baker (Wildlife Conservation Research Unit, Department of Zoology, University of Oxford, Recanati-Kaplan Centre, Tubney House, OX13 5QL, UK)

Stephen A. Ellwood (Department of Zoology, University of Oxford. OX13 3SZ, UK)

10 Jens Tronicke (Institut für Erd- und Umweltwissenschaften, Universität Potsdam, Karl-Liebknecht Straße 24, 14476 Potsdam, Germany)

- Corresponding Author (Niklas.Allroggen@geo.uni-potsdam.de)

15 Abstract

Ground-penetrating radar (GPR) is widely applied to provide highly resolved images of subsurface sedimentary structures, with implications for processes active in the vadose zone. Frequently overlooked among these structures are tunnels excavated by fossorial animals (e.g. moles). We present two repeated GPR surveys collected a year
20 apart in 2016 and 2017. Careful 3D data processing reveals, in each dataset, a pattern of elongated structures which are interpreted as a subsurface mole tunnel network. Our data demonstrate the ability of 3D GPR imaging to non-invasively image small animal tunnels (~5cm diameter), at a higher spatial and geolocation resolution than has previously been achieved. In turn this makes repeated surveys and therefore long
25 term monitoring, possible. Our results offer valuable insight into the understanding of the near surface and showcase a potential new application for geophysical methods as well as a non-invasive method of ecological surveying.

Introduction

30 Ground-penetrating radar (GPR) is a standard geophysical tool which provides high resolution imaging of the shallow subsurface (Bristow et al. 2003; Daniels 2005). Frequently overlooked in GPR processing and interpretation are shallow structures such as tunnels excavated by fossorial animals. While potentially only centimetre-scale in diameter, a single, interconnected tunnel network for some species may
35 extend over several hundred metres and can therefore contribute to the macropores

influencing subsurface hydrology (e.g., Blouin et al. 2013; Reck et al. 2018), or destabilize embankments and other earthworks (e.g., Di Prinzio et al. 2010; Borgatti et al. 2017). Consequently, any ability to accurately map animal tunnels improves the understanding both of shallow hydrological structure and, critical to this paper, animal
40 ecology.

GPR is especially suitable for imaging the tunnels of fossorial animals, due both to its high resolution and rapid data acquisition capability. Although GPR has been applied for imaging and locating small-scale subsurface tunnel networks of fossorial animals (e.g. Stott, 1996; Cortez et al. 2013; Chlaib et al. 2014; Saey et al. 2016), its ability to
45 monitor their development over time has not yet been demonstrated. Compared to other techniques for mapping tunnels, e.g., the excavation of a tunnel network (Šklíba et al. 2012), GPR is minimally invasive and leaves the tunnel network intact such that there is no disturbance to animal activities. Consequently, repeated surveys make it possible to image the evolution of the tunnel network over time, and thereby monitor
50 subsurface animal activity.

In this paper, we consider the application of GPR for monitoring feeding tunnels excavated by the European mole (*Talpa europaea*). Moles live almost entirely underground in a network of underground feeding tunnels. They excavate and then maintain the tunnels, depositing spoil heaps (or 'molehills') as they dig. For most of
55 the year moles are solitary individuals living in largely exclusive home ranges (Macdonald et al. 1997), the size of which depend on resource quality and in the UK

have been measured to range between 300 and 3000 m² (Gorman & Stone, 1990). It is not therefore possible to estimate how many moles live in a given area based on geographical area or the number of molehills contained within it. During the
60 springtime breeding season male moles leave their usual range in search of females to mate with (Gorman & Stone, 1990; Baker et al. 2015). After giving birth, females raise their offspring and teach them to hunt. From about June, in the UK, juvenile moles leave the natal range and go in search of their own territory (Atkinson, 2012).

As a GPR target, mole tunnels are particularly challenging because their diameter is
65 only approximately 5 cm and their geometry can be complex. These tunnels therefore pose a novel imaging and monitoring application for high resolution GPR studies, requiring the highest precision while recording, geolocating and processing the GPR data.

Here, we present GPR surveys recorded in two consecutive years over mole tunnels at
70 a field site in Tubney, Oxfordshire, UK. After describing our data acquisition and processing approach, we interpret our results using specific data attributes. We present our data in the form of an energy-specific attribute that highlights a complex network of connected subsurface features, which were validated as mole tunnels by excavation of a test pit. We therefore demonstrate that, by applying a modern survey
75 approach, GPR possesses the accuracy to monitor shallow subsurface targets with even the challenging complexity of a mole tunnel.

Methods

80 **Survey site and data acquisition**

To evaluate the feasibility of GPR to image and monitor mole tunnels, we selected a test site where significant mole activity has been observed for several years. Our survey site is a grassed lawn, with no significant topographic variation (Figure 1), in the grounds of a historic house in Tubney, Oxfordshire, UK. The uppermost subsurface
85 at our field site consists of a uniform sandy soil with a high content of organic material. The two surveys were conducted approximately 12 months apart, on 22.11.2016 and on 05.12.2017. They involved the collection of 3D GPR data within a 6 m x 18 m area. Autumn was chosen for our study because mole tunnelling activity and consequent production of molehills (spoil heaps) peak twice annually in the UK, in the
90 spring and autumn (Baker et al. 2016). By choosing autumn we wanted to maximise the presence of fresh excavations while avoiding any potential disturbance of the moles during their spring breeding period. The weather conditions during both surveys were cold (~5° C air temperature) and wet; there was rainfall around both periods, although not specifically while the second survey was taking place.

95



Figure 1: Photograph of our field site in West Oxfordshire, UK. The photograph is taken immediately after the completion of the 2016 3D GPR survey, and before undertaking the ground-truthing excavation.

100

All GPR data were recorded using a Sensors&Software PulseEKKO PRO system, equipped with a 1000 MHz transmitter antenna and a 500 MHz receiver antenna. Although this setup was originally forced because of a system failure during the first survey, it ultimately provided good results and was therefore used again for the
105 second survey. This observation is consistent with the previous studies of Mellett (1995), which showed that a set of bistatic antennas with different central frequencies but an overlapping total bandwidth, can provide better results than a setup in which the antennas share a common centre frequency. Antennas were fixed at a constant offset of 0.2 m, and traces were discretised into a sampling interval of 0.05 ns.

110 To locate the GPR traces, we employed a kinematic surveying strategy that combined
our GPR system with a self-tracking total station (Leica TPS 1200), providing positional
information with accuracy better than 0.01 m (Böniger and Tronicke 2010b). With this
setup, both 3D GPR datasets were acquired with an in- and cross-line trace spacing of
~1 cm and ~5 cm, respectively. Based on previously reported case studies (e.g.,
115 Allroggen et al. 2015), reliable time-lapse signatures can only be obtained where such
careful survey design and data acquisition protocols are employed, especially when
the target structures are close to the resolvable limit of GPR reflection data.

For additional velocity control and zero-time analyses, and after an initial pass of data
imaging, we collected a common-midpoint (CMP) survey over a region of the lawn not
120 thought to contain a tunnel (based on a lack of molehills and other surface signs). This
survey used minimum and maximum source-receiver offsets of 0.2 m and 1.5 m,
respectively, with stepwise offset increments of 0.04 m.

125 **Data processing**

The flowchart in Figure 2 shows our basic processing sequence. First, we applied a
background removal filter to each recorded 2D GPR profile to suppress direct arrivals
and subsequent ringing events. Then, to further improve the signal-to-noise ratio of
our data, we applied a Butterworth bandpass filter with cut-off frequencies of 500
130 MHz and 1500 MHz. Thereafter, we applied a natural neighbour gridding routine

(Sambridge et al. 1995) to interpolate the recorded GPR traces from their irregular recording locations to a regular grid, with a node spacing of 0.02 m in both in- and cross-line directions.

Parameters for further processing steps, including zero-time correction and Kirchhoff migration, were estimated from common midpoint (CMP) data collected in 2016 (not
135 shown) and 2017. Figure 3 shows the CMP records collected in December 2017, after bandpass filtering and amplitude scaling, acquired immediately adjacent to the 3D GPR surveying field.. CMP gathers were acquired both to determine GPR velocity and to compare the approach of using a transmitter/receiver pair of different frequency.
140 Figures 3a/b show CMP data and the semblance-based velocity spectrum using the typical setup of two 1000 MHz antennas, with Figures 3c/d showing the equivalent for our approach of a 1000 MHz transmitter and a 500 MHz receiver.

Due to the lack of clear reflected arrivals in Figure 3b, we did not interpret velocity information from this survey. On the contrary, Figure 3d shows a rather constant
145 subsurface velocity distribution and a reflection event that expresses a velocity of ~ 0.08 m/ns. Consequently, we use a constant GPR propagation velocity of 0.08 m/ns ($\epsilon_r = 14$) for further processing. Furthermore, these spectra validate our combination of a 500 MHz receiver with a 1000 MHz transmitter, with data quality being superior to that from the more typical setup of a 1000 MHz antenna pair.

150 The time-zero information derived from the CMP survey was also applied to correct time-zero in each GPR trace. Thereafter, we applied a scaling function based on the

average envelope calculated for each 3D GPR data set. Although such a scaling strategy prevents quantitative amplitude analysis, it preserves the relative amplitude changes within each data set. To remove steeply dipping events related to, e.g., diffraction tails, we applied a 3D frequency-wavenumber (f_k)-filter. Finally, migration was applied using a 3D Kirchhoff algorithm (Allroggen et al. 2015) with the assumption of a constant velocity of 0.08 m/ns ($\epsilon_r = 14$).

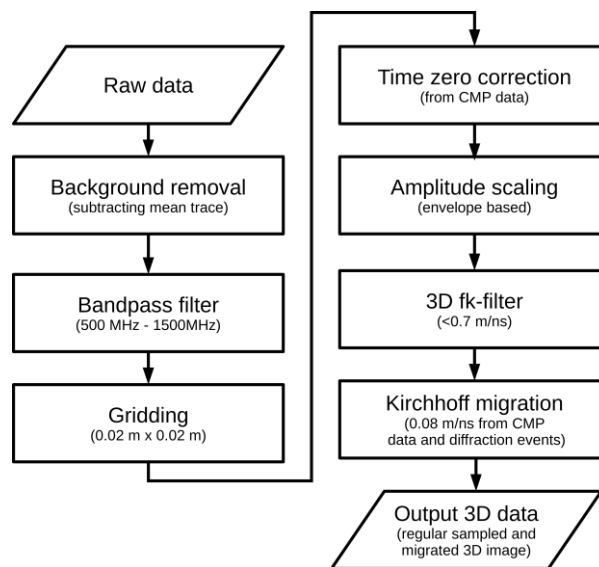
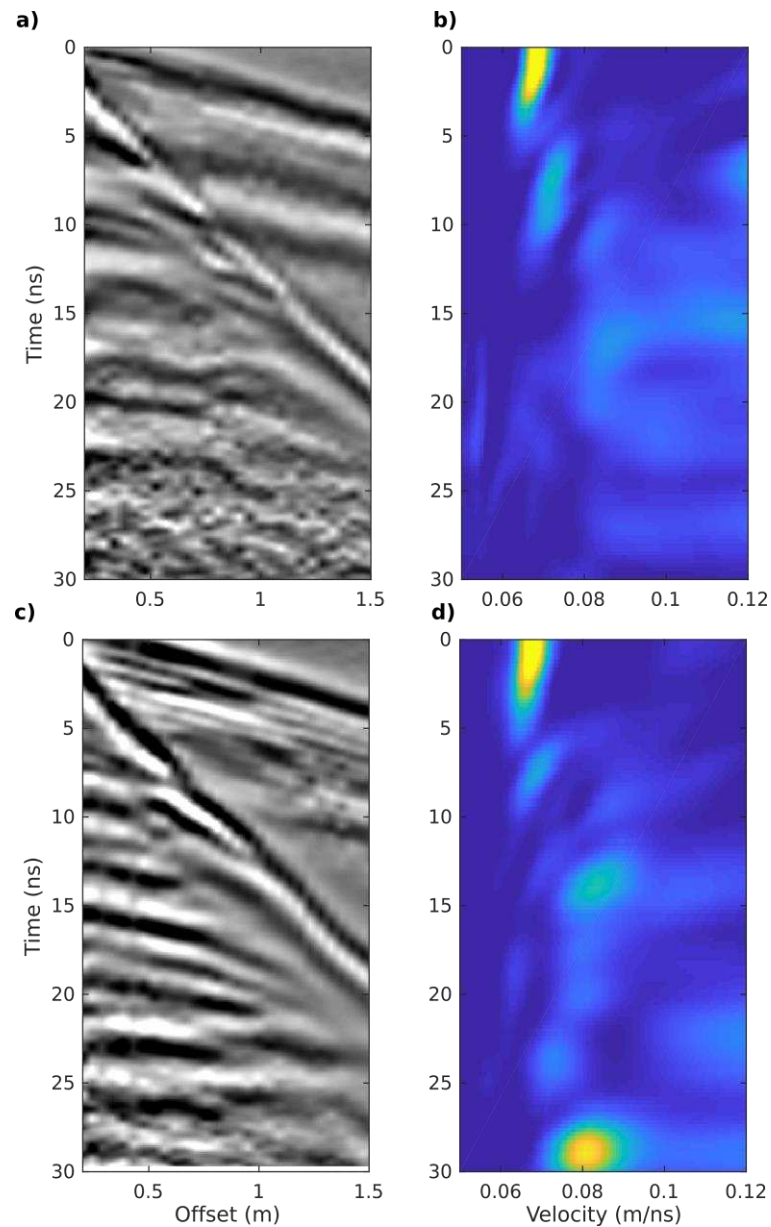


Figure 2: GPR processing sequence as applied to both 3D GPR data sets. Processing steps, such as background removal and envelope-based amplitude scaling, were necessary to improve data quality, but prevent a detailed trace-to-trace comparison of the individual time steps.

By applying the presented processing sequence to both 3D GPR datasets, we obtained two collocated data volumes, allowing: a) 3D imaging and delineation of shallow

subsurface structures, and b) interpretation of changes between the 2016 and 2017 surveys. However, it should be noted that processing steps such as background removal and amplitude scaling prevent a quantitative comparison of the amplitudes of collocated traces and, thus, limit our interpretation to a qualitative comparison of

170 observed structures.



175

Figure 3: Co-located CMP surveys acquired in November 2017, for velocity measurement and comparing data quality with different antenna sets. a) CMP survey data recorded at the same position in November 2017 using a pair of 1000 MHz Sensors&Software PulseEKKO Pro antennas and b) Velocity spectrum of (a) showing no interpretable reflection energy. c) CMP survey data recorded with a 1000 MHz
 180

transmitter antenna and a 500 MHz receiving antenna and d) Velocity spectrum of (c), indicating a constant GPR propagation velocity of ~ 0.08 m/ns at ~ 15 ns traveltime.

Results

185 A selected GPR profile is extracted from the same position in the 2016 (Figure 4a) and 2017 (Figure 4b) datasets, showing GPR responses at a crossline distance of 1.85 m (as highlighted in Figure 5). In the panels of Figure 4, both profiles show subsurface structures up ~ 25 ns travel-time, corresponding to a depth of ~ 1 m with the assumed velocity of 0.08 m/ns ($\epsilon_r = 14$). Numerous consistent reflection events can be
190 identified in them (e.g., the rather continuous reflection pattern between ~ 15 - 25 ns travel-time at an inline distance of ~ 7 m), but significant structural differences between the two profiles are also evident, especially at travel times < 5 ns.

From an interpretational point of view, we expect two classes of subsurface structures, namely mole tunnels and soil structures representing the geological
195 background. While mole tunnels are limited in diameter (~ 0.05 m) and expected to form an irregular, partly dynamic network predominately in the uppermost decimetres of the subsurface, the geological background structure might be represented by a variety of static structures at different spatial scales of heterogeneity. Obviously, a single 2D GPR profile is not sufficient to distinguish mole
200 networks from the geological background. Thus, our structural interpretation (as indicated in Figure 4) relies on a strategy where our data are visualized and

interpreted in 3D using time slices and fence diagrams. This allows the identification of larger-scale geological structures and network-like tunnel systems (e.g., those labelled in Figure 4).

205 The visibility of the mole tunnel was further enhanced by testing and generating specific data attributes, known from GPR experience elsewhere (e.g., Böniger and Tronicke 2010a) to be suitable for highlighting subtle features. Figure 5 shows an energy attribute calculated from a time-averaged envelope within a user-specified time-window, here between 2 ns and 4 ns (~ 0.08 and ~ 0.16 m), corresponding to a
210 depth window where mole activity was expected to be concentrated after an initial inspection of the data. The attribute slice is further enhanced, preserving relevant structural scales while suppressing random noise and spikes, using a 3x3 median filter. In the resulting time slices (Figures 5a and 5b) high energies indicate network-like structures, interpreted as tunnels built and adapted by moles.

215

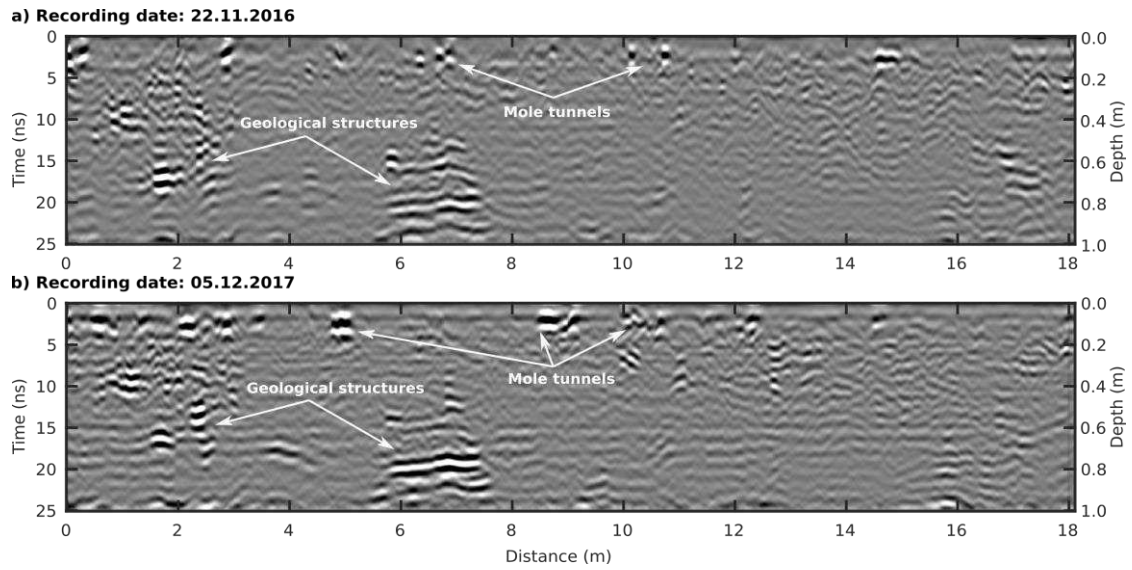


Figure 4: 2D GPR profiles extracted at a crossline distance of 1.85 m from: a) the 2016 survey and b) the 2017 survey. Depths are approximated using a constant velocity of 0.08 m/ns ($\epsilon_r=14$).

The interpretation of mole tunnels is supported by ground-truthing conducted immediately following the 2016 survey. We excavated a test pit measuring ~ 1 m x ~ 2 m in area (blue box in Figure 5a). The excavation revealed a mole tunnel with several
230 branches at a depth between ~ 0.05 m and ~ 0.25 m (Figure 6), which we mapped using a total station; the mapped positions are shown as reference points in Figure 5a (red dots within the blue box). The ground-truth tunnel geometry is in agreement with the location of a tunnel-like structure interpreted in our GPR time slice (Figure 5a). However, amplitude variations along the tunnel trajectories complicate a detailed and
235 reliable segmentation of the tunnel network. A possible explanation for these amplitude variations, which are difficult or even impossible to quantify, include variations in antenna coupling and radiation patterns, energy variations due to varying absorption, or changes in depth and diameter of the tunnel network.

240 When comparing the time slices in Figure 5a and 5b, we observe both changes and similarities in the network between the 2016 and 2017 surveys. To simplify the interpretation, we compare our interpretation of the individual surveys in Figure 5c and distinguish between tunnels only visible in 2016 (green lines), novel tunnels in 2017 (red lines) and persistent tunnels in both years (blue lines). For example, the
245 ring-like structure between inline distances of ~ 8 m and ~ 12.1 m and crossline distances between ~ 2 m and ~ 4.1 m is consistent between both datasets, although there is a significant discrepancy in its shape in the upper right corner. Additionally,

the complexity – expressed here by the number of junctions – of the tunnel network with the ring structure increases between 2016 and 2017 surveys. In contrast, the area excavated in 2016 shows no mole activity into the 2017 period. Here the moles have created two new tunnels, which connect the disturbed tunnels, but avoid the excavated area (Figure 5c).



Figure 6: Photograph showing the test pit containing a mole tunnel network across an area of ~ 1 m x ~ 2 m in a depth of ~ 0.1 m below ground surface. After taking the image, the soil pit was extended down to a depth of ~ 0.6 m with no further evidence of deeper tunnels observed.

Discussion and conclusions

Our results demonstrate that GPR is well suited to mapping small anomalies such as the tunnels of small animals. It provides a non-invasive method for mapping tunnel systems (and consequently aspects of animal behaviour) that are otherwise difficult to

study; this has previously been done by excavating and therefore destroying tunnel systems, or by tracking the animals themselves. Importantly, the ability to accurately align the results of consecutive studies allows investigation of the development of tunnel systems over time, something that is clearly impossible using destructive methods of tunnel mapping (Skliba et al. 2012), while animal tracking is invasive because it requires animal capture and device attachment (e.g., Skliba et al. 2009).

The resulting data show exciting and novel insights into the development of subsurface structures. Nevertheless, interpretation is so far limited to the imaging of soil structures and further methodological development is necessary to a) distinguish actual mole tunnels from comparable structures including geological background reflections, (e.g., root systems, man-made structures and buried utilities); and b) extract quantitative information on tunnel diameter from the character of diffraction hyperbolae (e.g., Dou et al. 2017). GPR is not yet able to distinguish used and unused tunnels, although monitoring at finer temporal intervals would enable a more detailed description of the gradual evolution of the tunnels and thus the activity of the animal. In addition, our approach might also help to distinguish animal-related structural changes from other dynamic processes, such as those related to soil moisture variations.

We conclude that an approach to GPR surveying which focuses on very high spatial and geolocation resolution provides an opportunity to image and monitor both the spatial and temporal 3D tunnelling activity of small fossorial animals. Considering the

small size of the target structures (tunnels with diameters ~5 cm), we found that
285 careful survey design, a data acquisition that includes high-precision positional
information, plus a target-oriented processing and interpretation strategy, are
indispensable. We anticipate that the presented approach, following high resolution,
repeatable and non-invasive 3D GPR imaging, will improve our understanding of the
shallow subsurface and the behaviour of small tunnelling animals that otherwise are
290 difficult to study objectively and non-invasively.

References

- Allroggen N., Tronicke J., Delock, M. and Böniger U. 2015. Topographic migration of
2D and 3D ground-penetrating radar data considering variable velocities. *Near*
295 *Surface Geophysics* 13(3), 253–259.
- Allroggen N., van Schaik N.L.M.B. and Tronicke J. 2015. 4D ground-penetrating radar
during a plot scale dye tracer experiment. *Journal of Applied Geophysics* 118,
139-144.
- Atkinson, R. P. D. 2012. *Moles; The British Natural History Collection, Volume 3.*
300 Whittet Books (Publishers), Stansted, Essex, UK.
- Baker S.E., Ellwood S.A., Johnson P.J. and Macdonald D.W. 2016. Moles and mole
control on British farms, amenities and gardens after strychnine withdrawal.
Animals 6(6), 39. Special edition on: Ethical and Welfare Dimensions of the
Management of Unwanted Wildlife.

- 305 Baker, S. E., Shaw, R. F., Atkinson, R. P. D., West, P. & Macdonald, D. W. (2015)
Potential welfare impacts of kill-trapping European moles (*Talpa europaea*) using
scissor traps and Duffus traps: a post-mortem examination study. *Animal Welfare*
24, 1-14.
- Blouin M., Hodson M. E., Delgado E. A., Baker G., Brussaard L., Butt K. R., Dai J.,
310 Dendooven L., Peres G., Tondoh J.E., Cluzeau D., Brun J. J. 2013. A review of
earthworm impact on soil function and ecosystem services. *European Journal of*
Soil Science 64(2), 161–182.
- Böniger U. and Tronicke J. 2010a. Improving the interpretability of 3D GPR data using
315 target-specific attributes: application to tomb detection. *Journal of Archaeological*
Science 37, 672-679.
- Böniger U. and Tronicke, J. 2010b. On the potential of kinematic GPR surveying using
a self-tracking total station: evaluating system crosstalk and latency. *IEEE*
Transactions on Geoscience and Remote Sensing 48, 3792–3798.
- 320 Borgatti L., Forte E., Mocnik A., Zambrini R., Cervi F., Martinucci D., Pellegrini F.,
Pillon S., Prizzon A., Zamariolo, A. 2017. Detection and characterization of
animal burrows within river embankments by means of coupled remote sensing
and geophysical techniques: Lessons from River Panaro (northern Italy).
Engineering Geology 226, 277–289.
- 325 Bristow, C. S., & Jol, H. M. 2003. *Ground penetrating radar in sediments*. London: The
Geological Society of London.

- Chlaib H. K., Mahdi H., Al-Shukri H., Su M. M., Catakli A. and Abd, N. (2014). Using ground penetrating radar in levee assessment to detect small scale animal burrows. *Journal of Applied Geophysics* 103, 121–131.
- 330 Cortez J. D., Henke S. E., Redeker E., Fulbright T. E., Riddle R. and Young, J. 2013. Demonstration of ground-penetrating radar as a useful tool for assessing pocket gopher burrows. *Wildlife Society Bulletin* 37(2), 428–432.
- Daniels, D. J. 2005. *Ground penetrating radar* (2nd ed.). London: Institution of Engineering and Technology.
- 335 Dou Q., Wei L., Magee D. and Cohn A. 2017. Real-time hyperbolae recognition and fitting in GPR data. *IEEE Transactions on Geoscience and Remote Sensing* 55(1), 51-62.
- Di Prinzio M., Bittelli M., Castellarin A. and Pisa P. R. 2010. Application of GPR to the monitoring of river embankments. *Journal of Applied Geophysics* 71(2–3),
340 53–61.
- Gorman, M. L. and Stone, R. D. 1990. *The Natural History of Moles*. Christopher Helm (Publishers), Bromley, Kent, UK.
- Macdonald, D. W., Atkinson, R. P. D. and Blanchard, G. 1997. Spatial and temporal patterns in the activity of European moles. *Oecologia* 109, 88-97.
- 345 Mellett J. S. 1995. Use of bistatic in ground-penetrating alloffrequency antennas radar (GPR) investigations. In *Symposium on the Application of Geophysics to Engineering and Environmental Problems 1995*, 405–411.

- Reck A., Jackisch C., Hohenbrink T. L., Schröder B., Zangerlé A. and van Schaik L.
2018. Impact of Temporal Macropore Dynamics on Infiltration: Field Experiments
350 and Model Simulations. *Vadose Zone Journal* 17, 170147.
- Saey T., Van Meirvenne M., De Pue J., Van De Vijver E. and Delefortrie S. 2014.
Reconstructing mole tunnels using frequency-domain ground penetrating radar.
Applied Soil Ecology 80, 77–83.
- Sambridge M., Braun J. and McQueen H. 1995. Geophysical parametrization and
355 interpolation of irregular data using natural neighbours. *Geophysical Journal
International* 122(3), 837–857.
- Šklíba J., Mazoch V., Patzenhauerová H., Hrouzková E., Lövy M., Kott O. and
Šumbera R. 2012. A maze-lover's dream: Burrow architecture, natural history and
habitat characteristics of Ansell's mole-rat (*Fukomys anelli*). *Mammalian*
360 *Biology* 77(6), 420–427.
- Skliba J., Šumbera R., Chitaukali W.N. and Burda H. 2009. Home-Range Dynamics in
a Solitary Subterranean Rodent. *Ethology* 115, 217-226.
- Stott P. 1996. Ground-penetrating radar: A technique for investigating the burrow
structures of fossorial vertebrates. *Wildlife Research* 23(5), 519–530.

365